doi:10.3772/j.issn.1006-6748.2019.04.013

# Wind disturbance rejection control based on the dynamic parameters estimation of quadrotors UAV①

Yang Yanhua (杨艳华)②, Chen Yang

(School of Information Science and Engineering, Wuhan University of Science and Technology, Wuhan 430081, P. R. China)

(Engineering Research Centre for Metallurgical Automation and Measurement Technology of Ministry of Education, Wuhan 430081, P. R. China)

**Abstract**

The turbulence or gust in quadrotor flight environment causes drastic changes in the unmanned aerial vehicle (UAV) aerodynamic parameters. Especially, rotor thrust coefficient and reaction torque coefficient of the UAV encounter uncertainty fluctuation, which may undermine the control performance. A real-time estimation strategy for these aerodynamic parameters is proposed to improve the identification on the disturbance. First, the unscented Kalman filter (UKF) algorithm is used to estimate the UAV states and aerodynamic parameters. Then, a double-loop structure, consisting of position and attitude, is designed for the trajectory tracking control. In the outer loop, a proportional-derivative controller is adopted to carry out position tracking and provide Euler angle references for the inner loop, called attitude controller. Moreover, the attitude controller is designed using an inverse dynamic technique. The main contribution of this study is to propose a joint estimation on the aerodynamic parameters with wind disturbance as well as the UAV states. This strategy plays an important role in refining time-varying parameters of wind disturbance. A number of simulations are executed to verify the effectiveness of the proposed method.

**Key words**: unscented Kalman filter (UKF), joint estimation, wind disturbance, unmanned aerial vehicle (UAV), quadrotor

## 0 Introduction

In recent years, quadrotor unmanned aerial vehicle (UAV) has become one of the hotspots in the field of robot research. Quadrotor is a promising device for its advantages with vertical takeoff and landing, movement agility, and low cost, some application can be seen in the aerial photography, resource survey, material delivery, and so on[1,2]. However, the wind turbulence such as gust in the actual flying environment will frequently lead to deterioration of the control performance of the UAV. This kind of external disturbance creates a huge level of uncertainty for the UAV[3]. As a result, it is difficult for the quadrotor generally to track the expected path or trajectory, even lose its destination and gives rise to some disasters. In this work, a contribution is made to this practical problem and a control strategy is proposed for the wind disturbance rejection of quadrotor.

Some researchers have studied the quadrotor flight control with the wind turbulence[4-9]. There are 2 main methods in the literature. One is the utilization of the aerodynamic theory to parameterize the wind modeling, and the commonly used models include the Dryden turbulence model and the Von Karman wind field model. For example, Hancer et al[4] studied the robust position control problem with wing pitch input for a Tilt-Wing Quadrotor. Based on the Dryden turbulence model, they considered the external wind disturbance as the sum of multiple sine functions with multiple parameters, i.e., amplitude, frequency and phase that can be estimated by online observers. A simplified potential field was used in Sydney et al[5] to model the wind disturbance. With the help of the measured ground speed and wind speed online, the parameters are recursively updated with Bayesian estimation. Finally, the feedback linearization technique was adopted to design the controller. The wind disturbance model established by Waslander et al[6] was composed of static

① Supported by the National Natural Science Foundation of China (No. 61703314, 61573263) and National Key Research and Development Program of China (No. 2017YFC0806503).

② To whom correspondence should be addressed. E-mail: yangyh@wust.edu.cn.

Received on Dec. 21, 2018

wind model and gust model, and the latter used standard power spectral density function. In order to improve the positioning accuracy of the UAV, they designed a wind speed compensator to reduce the uncertainty of the position feedback control. Similarly, Escareño et al[7] studied the horizontal wind disturbance problems, and put forward a hierarchical control structure, in which an adaptive controller was designed for the static (time-invariant) wind disturbance while for the time-varying wind disturbance, the parametric model was established based on the sine function. Wang et al[8] first established a multiple-parameters wind disturbance model and then established a double closed-loop control structure for the quadrotors. The outer loop adopted robust adaptive backstepping controller for the wind turbulence parameters estimation, and the inner loop used the global sliding mode controller to achieve the steady attitude control of the quadrotor. These methods are usually based on the stochastic nonlinear theory. Besides, the wind disturbance model is calculated under various general conditions and assumptions that might cause these methods infeasible in the real application.

The other is the method of online identification and estimation of the wind disturbance[10-14]. It usually does not have a known model of the wind disturbance, but it is assumed that the uncertainty of the UAV state is mainly caused by wind disturbance. So, the designed controller is updated by the real-time estimation of the UAV states in order to achieve effective control in the case of the wind disturbance. Rigatos et al[10] firstly linearized the nonlinear control system model using the differential flat theory and then designed the derivative-free nonlinear Kalman filter to estimate the state. Finally, a disturbance observer was designed for the quadrotor UAV control. Nobahari et al[11] used continuous ant colony filters to perform on-line quadrotor state estimation and ground effect compensation and then designed an effective altitude controller. Mercado et al[12] used extended Kalman filter (EKF) to estimate the position and velocity of the quadrotor UAV. A proportional-derivative controller and a second-order sliding mode controller were designed for the translational and rotational motion, respectively. Then, simulation results showed that their method can be used to deal with the external disturbance and the measurement uncertainty. This kind of method regards the quadrotor UAV control under wind disturbance as the uncertainty problem and tries to estimate the position and the attitude of the UAV to improve the controller performance.

This study also deals with the wind disturbance as a kind of uncertainty. However, it is held that it is the wind disturbance that causes the efficiency loss of the UAV rotors. The motivation is to find the factor reflecting the time-varying efficiency online. Exactly, there are 2 parameters, namely, thrust coefficient and reaction torque coefficient, denoting a kind of efficiency state, which are very sensitive to wind disturbance. These 2 parameters directly reflect the efficiency at certain operating point of UAV in the air. When gust of wind occurs, these 2 coefficients change drastically. In other words, it is through these efficiency states that the wind disturbance causes an effect on quadrotor UAV states.

Based on this view, not wind disturbance parameters or UAV states but wind disturbance impacts on the thrust and the reaction torque of the UAV are specified in this study. The impacts are reflected by model parameters, that is, the thrust coefficient and the reaction torque coefficient. However, in all existing literature, these parameters are known as unchangeable. On the contrary, they are treated as time-varying parameters. Therefore, this study proposes estimating them as well as some other states in the UAV model to track the changes in the environment in real time. Then, these new factors are used to update the controller in real time so as to achieve effective wind disturbance rejection control.

The parameters estimation method in this work is based on the unscented Kalman filter (UKF), which is a typical nonlinear parameter estimation algorithm. It has the advantages of small computation and good real-time performance. In the field of the UAV control, this algorithm is often used to estimate fault parameters for improving the fault tolerance and safety. For example, Izadi et al[15] studied the UAV driver fault who formulated a fault estimator with moving Horizon estimation and the UKF algorithm. The UKF algorithm is also used for visual tracking control[16], force and moment estimation[17].

In this work, the model parameters, the thrust coefficient, and the reaction torque coefficient, which are related to the wind disturbance, are directly added as state variables. UAV states, as well as the newly added efficiency factors, make up the augmented states that will be estimated synchronously under the same UKF framework. Next, an embedded control structure and controllers, including the proportional-derivative (PD) controller and the inverse dynamic controller (IDC), are designed for the UAV steady flight. This paper is arranged as follows. Section 1 introduces the online estimation of the quadrotor UAV model parameters. Section 2 demonstrates the simulation experiment and comparative analysis, and finally, a brief conclusion is given in Section 3.

## 1 Parameters estimation for quadrotor UAV model

### 1.1 Quadrotor UAV model

A prototype of the quadrotor UAV is shown in Fig. 1(a). The coordinate system attached to the UAV body and the north-east-down (NED) inertial coordinate system is drawn according to the UAV mass center in Fig. 1(b). There are 4 real inputs for this machine, defined as $f_i$, $i = 1, 2, 3, 4$, respectively, representing the thrust force generated by the 4 motor rotations. As shown in Fig. 1, the order of the motors is defined as $M_1$ and $M_2$ which are located in the positive direction of the $x$ and $y$ axes (front and right), respectively, and $M_3$ and $M_4$ are located in the negative direction of the $x$ and $y$ axes (rear and left), respectively. The quadrotor UAV flying in the air has a total of 6 degrees of freedom, including 3 translational movements and 3 rotations around the axes. Since the number of control inputs is less than that of degrees of freedom, quadrotor UAV is a typical under-actuated system.

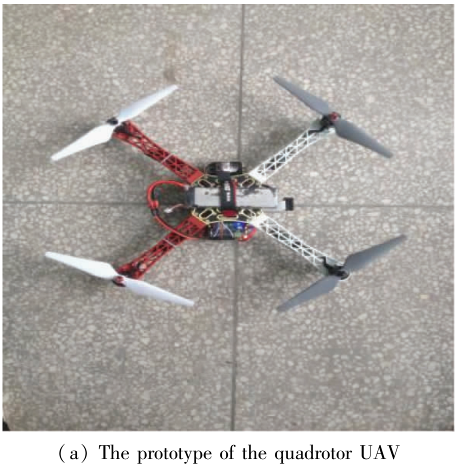

(a) The prototype of the quadrotor UAV

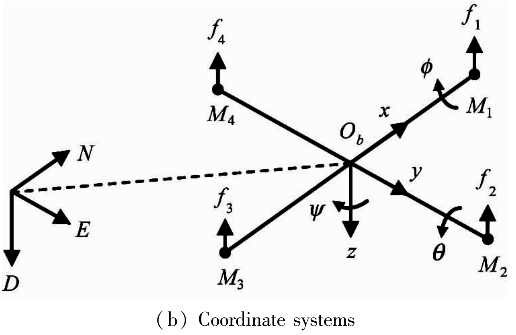


(b) Coordinate systems

**Fig. 1** Quadrotor UAV and the coordinate systems

Define the Euler as follows: the roll angle of the UAV rotating around the $x$-axis of its body system is denoted by $\phi$. The pitch angle $\theta$ represents the angle that the UAV rotates around the $y$-axis and the heading angle, $\psi$, represents the angle that the UAV rotates around the $z$ axis. In contrast to the inertial coordinate system, if the vehicle rotates following the order of the $z$-axis, the $y$-axis, and the $x$-axis and gets rotation angles $\psi$, $\theta$, $\phi$, then the matrix calculated from the body coordinate system to the inertial coordinate system is [18]:

$$\boldsymbol{R}_T = \begin{bmatrix} C_\psi C_\theta & S_\psi C_\theta & -S_\theta \\ C_\psi S_\theta S_\phi - S_\psi C_\phi & S_\psi S_\theta S_\phi + C_\psi C_\phi & C_\theta S_\phi \\ C_\psi S_\theta C_\phi + S_\psi S_\phi & S_\psi S_\theta C_\phi - C_\psi S_\phi & C_\theta C_\phi \end{bmatrix} \tag{1}$$

The rotation of the 4 motors together produces a total thrust of the UAV and regulates the motors' speed to lead to a variety of movements which is listed in Table 1[19]. Since the motors $M_1$ and $M_3$ in Fig. 1 rotate counterclockwise while $M_2$ and $M_4$ rotate clockwise, this arrangement eliminates the possible yawing moment caused by the aerodynamic reaction torque of the UAV.

According to the aerodynamics theory, the thrust force $f_i$ and the rotational inertia generated by each rotor are proportional to the square of its speed, and the input variables are defined as

$$F_i \triangleq \omega_i^2, \quad i = 1,2,3,4. \tag{2}$$

where $\omega_i$ is the rotational angular velocity of the rotor $i$ and $f_i \propto F_i$. According to the operating characteristics of the quadrotor UAV, the virtual control variables $\boldsymbol{U} = [U_1, U_2, U_3, U_4]^{\mathrm{T}}$ are defined as

$$\begin{cases} U_1 = b(F_1 + F_2 + F_3 + F_4) \\ U_2 = b(-F_2 + F_4) \\ U_3 = b(F_1 - F_3) \\ U_4 = d(F_1 - F_2 + F_3 - F_4) \end{cases} \tag{3}$$

where $U_1$, $U_2$, and $U_3$ represent the pseudo control variables for UAV generating lifting, rolling, pitching motion respectively. $U_4$ is the pseudo-variable to control the desired heading. $b$ is the thrust coefficient, which is a parameter mainly determined by the size and configuration of the rotor. $d$ is the reaction torque coefficient. Assuming that the quadrotor UAV is a 6-degree-of-freedom rigid body, its dynamics can be deduced using the Newton-Euler method[20]:

$$\dot{X} = f(\boldsymbol{X}, \boldsymbol{U}) \tag{4}$$

where, the state variables are

$$\boldsymbol{X} = [\phi \quad \dot{\phi} \quad \theta \quad \dot{\theta} \quad \psi \quad \dot{\psi} \quad z \quad \dot{z} \quad x \quad \dot{x} \quad y \quad \dot{y}]^{\mathrm{T}} \tag{5}$$

$$f(\boldsymbol{X},\ \boldsymbol{U}) = \begin{bmatrix} x_2 \\ a_1 x_4 x_6 + b_1 U_2 \\ x_4 \\ a_2 x_2 x_6 + b_2 U_3 \\ x_6 \\ a_3 x_2 x_4 + b_3 U_4 \\ x_8 \\ g - \dfrac{U_1}{m}\cos x_1 \cos x_3 \\ x_{10} \\ -\dfrac{U_1}{m}(\sin x_1 \sin x_5 + \cos x_1 \sin x_3 \cos x_5) \\ x_{12} \\ \dfrac{U_1}{m}(\sin x_1 \cos x_5 - \cos x_1 \sin x_3 \sin x_5) \end{bmatrix} \tag{6}$$

As in traditional methods, the quadrotor structure is assumed rigid and symmetrical. The above dynamics is derived based on UAV hover flight and by neglecting the propellers gyroscopic effect resulting from the rotation. For convenience, $x_i = X(i)$ in Eq. (6) is introduced. The model parameters are $a_1 = \dfrac{I_y - I_z}{I_x}$, $a_2 = \dfrac{I_z - I_x}{I_y}$, $a_3 = \dfrac{I_x - I_y}{I_z}$, $b_1 = \dfrac{L}{I_x}$, $b_2 = \dfrac{L}{I_y}$, $b_3 = \dfrac{1}{I_z}$. Here, $m$ is the mass of the vehicle, $g$ is the acceleration of gravity, $L$ is the arm length of the quadrotor UAV. $I_x$, $I_y$, and $I_z$ are the inertia of $x$-axis, $y$-axis, and $z$-axis, respectively.

### 1.2 The structure of the quadrotor UAV control system

A double-loop control structure, as shown in Fig. 2, is adopted in this work. This structure consists of 2 subsystems, i. e., position control subsystem and attitude control subsystem. The outputs of the position subsystem are the references of Euler, $\phi_r$ and $\theta_r$, which are utilized as the inputs of the attitude subsystem. PD controller and IDC controller are designed for them respectively. The real states of the quadrotor UAV are estimated by the nonlinear estimation algorithm, named UKF.

Table 1 UAV motion related to the variations of the motors' speed

| Motion \ Motor | $M_1$ | $M_2$ | $M_3$ | $M_4$ |
|---|---|---|---|---|
| Rising motion | increasing | increasing | increasing | increasing |
| Descending motion | decreasing | decreasing | decreasing | decreasing |
| Rolling motion | - | increasing/decreasing | - | decreasing/increasing |
| Pitching motion | increasing/decreasing | - | decreasing/increasing | - |
| Yawing motion | increasing/decreasing | decreasing/increasing | increasing/decreasing | decreasing/increasing |

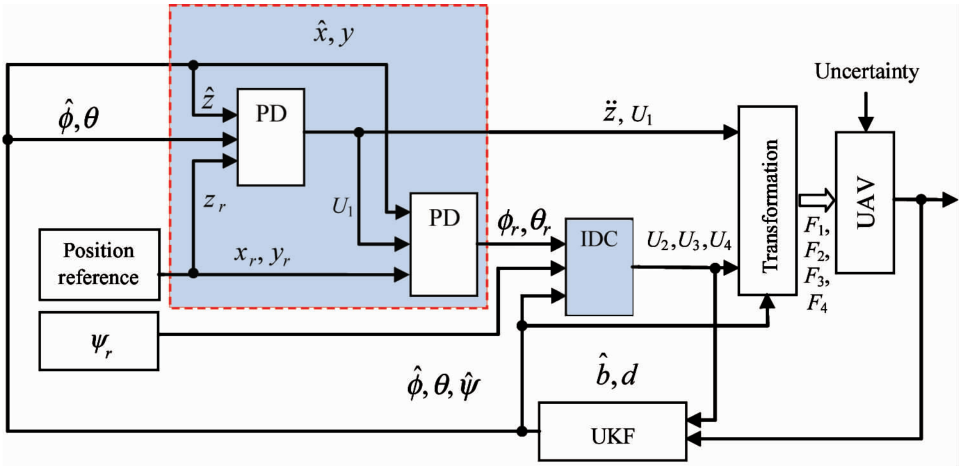


**Fig. 2** The proposed structure for quadrotor UAV control system

The dashed box in Fig. 2 denotes a PD controller for position subsystem designed using the UAV position feedback information. The subsequent IDC controller not only uses the output information of the PD controller but also uses the estimation result of the real-time feedback of the UKF algorithm, to calculate the real-time controller, $U_2$, $U_3$, and $U_4$.

### 1.3 Joint estimation of state and parameter based on UKF

1.3.1 The augmented state

The UAV state will change when the quadrotor UAV encounters gusts or other similar turbulence. It is assumed that it is the emergence of gusts and turbulence that causes the fluctuation of the aerodynamic parameters in flight and then causes the efficiency fluctuation of the rotors, resulting in changes in the state.

As a critical aerodynamic parameter, thrust coefficient $b$ and reaction torque coefficient $d$ are the bridges between the UAV and the flight environment. Considering that the model parameters, $b$ and $d$, are greatly affected by the disturbance, it is proposed to be included in the state vector as a supplement for online real-time estimation. Building the following system:

$$\dot{X}_s = f_s(X_s, \boldsymbol{F}) \tag{7}$$

where the state after the expansion is $X_s = [\boldsymbol{X};\ b;\ d]$. The control variable is converted to the square of the motor speed $\boldsymbol{F}_i$. $\boldsymbol{F} = [\boldsymbol{F}_1\ \ \boldsymbol{F}_2\ \ \boldsymbol{F}_3\ \ \boldsymbol{F}_4]^{\mathrm{T}}$ from virtual control $\boldsymbol{U}$. The detail system is shown in Eq. (8). The transformation matrix from $\boldsymbol{U}$ to $\boldsymbol{F}$ is shown in Eq. (9).

$$f_s(X_s, \boldsymbol{F}) = \begin{bmatrix} x_2 \\ a_1 x_4 x_6 + b_1 x_{13}(-\boldsymbol{F}_2 + \boldsymbol{F}_4) \\ x_4 \\ a_2 x_2 x_6 + b_2 x_{13}(\boldsymbol{F}_1 - \boldsymbol{F}_3) \\ x_6 \\ a_3 x_2 x_4 + b_3 x_{14}(\boldsymbol{F}_1 - \boldsymbol{F}_2 + \boldsymbol{F}_3 - \boldsymbol{F}_4) \\ x_8 \\ g - \dfrac{x_{13}(\boldsymbol{F}_1 + \boldsymbol{F}_2 + \boldsymbol{F}_3 + \boldsymbol{F}_4)}{m}\cos x_1 \cos x_3 \\ x_{10} \\ -\dfrac{x_{13}(\boldsymbol{F}_1 + \boldsymbol{F}_2 + \boldsymbol{F}_3 + \boldsymbol{F}_4)}{m}(\sin x_1 \sin x_5 + \cos x_1 \sin x_3 \cos x_5) \\ x_{12} \\ \dfrac{x_{13}(\boldsymbol{F}_1 + \boldsymbol{F}_2 + \boldsymbol{F}_3 + \boldsymbol{F}_4)}{m}(\sin x_1 \cos x_5 - \cos x_1 \sin x_3 \sin x_5) \\ 0 \\ 0 \end{bmatrix} \tag{8}$$

$$\boldsymbol{F} = \begin{bmatrix} \boldsymbol{F}_1 \\ \boldsymbol{F}_2 \\ \boldsymbol{F}_3 \\ \boldsymbol{F}_4 \end{bmatrix} = \begin{bmatrix} \frac{1}{4b} & 0 & \frac{1}{2b} & \frac{1}{4d} \\ \frac{1}{4b} & -\frac{1}{2b} & 0 & -\frac{1}{4d} \\ \frac{1}{4b} & 0 & -\frac{1}{2b} & \frac{1}{4d} \\ \frac{1}{4b} & \frac{1}{2b} & 0 & -\frac{1}{4d} \end{bmatrix} \begin{bmatrix} \boldsymbol{U}_1 \\ \boldsymbol{U}_2 \\ \boldsymbol{U}_3 \\ \boldsymbol{U}_4 \end{bmatrix} \tag{9}$$

1.3.2 UKF estimation

The UKF algorithm is one of the optimal estimation algorithms based on the Kalman filter (KF) framework still depended on Gaussian distribution assumption. In fact, UKF is the extension of KF in the nonlinear system. The utilization of the unscented transformation makes it feasible and high efficient to obtain the mean of the UAV state propagated by the nonlinear equation. Two steps, denoting prediction and correction, are included in the algorithm, which estimates the mean and the variance of the system state respectively. After discretized with proper sampling rate, the nonlinear dynamics model of the quadrotor UAV in Eq. (8) is shown in Eq. (10).

$$\begin{cases} X_s(k+1) = f_s(X_s(k), F(k)) + w(k) \\ Y_s(k) = \boldsymbol{H} X_s(k) + v(k) \end{cases} \tag{10}$$

where $k$ represents time step. $Y_s(k)$ represents the state of the measured value. $\boldsymbol{H} = [\boldsymbol{I}_{12}\ \ 0\ \ 0]$ is the proper matrix with dimensions of $12 \times 14$. $\boldsymbol{I}_{12}$ is a unit matrix that has the dimensions of 12. $w(k)$ and $v(k)$ indicate the process noise and the measurement noise, respectively, both of which are Gaussian white noise, i.e., $w(k) \sim N(0, Q_w)$, $v(k) \sim N(0, Q_v)$. Here, the variances, $\boldsymbol{Q}_w$ and $\boldsymbol{Q}_v$, are positive definite matrix with dimensions of $14 \times 14$ and $12 \times 12$, respectively.

Typically, the sampling rate in Eq. (10) is 1 kHz for the following simulations.

The UKF algorithm includes:

1) Initialize prior mean $\bar{X}_s$ and variance $P_0$ of state vector $\boldsymbol{X}$. The prior mean of $b$ and $d$ are $b_0$ and $d_0$, measured offline without wind disturbance.

2) Construct symmetry set of discrete Sigma points near the priori mean of state vector $\boldsymbol{X}$.

3) Update state and calculate its variance based on the unscented transformation.

4) Update state and calculate its variance according to the measurement results.

The algorithm flow can be briefly described by the following expression.

$$\hat{X}_s(k) = f_{\mathrm{ukf}}(X_s(k), F(k), P(k), Q_w(k), Q_v(k)) \tag{11}$$

Where the estimated vector is:

$$\hat{\boldsymbol{X}}_s(k) =$$

$$[\hat{\phi} \quad \hat{\dot{\phi}} \quad \hat{\theta} \quad \hat{\dot{\theta}} \quad \hat{\psi} \quad \hat{\dot{\psi}} \quad \hat{z} \quad \hat{\dot{z}} \quad \hat{x} \quad \hat{\dot{x}} \quad \hat{y} \quad \hat{\dot{y}} \quad \hat{b} \quad \hat{d}]^{\mathrm{T}}_{(k)}$$

Since the unscented transformation is used to replace the general linearization as in KF, UKF algorithm is no longer necessary to calculate the Jacobian matrix. Therefore, it can be used to deal with the non-derivative dynamics and improve the computing accuracy, especially when calculating the statistics of the state variables. In the following simulations, the square root UKF algorithm is used to calculate the updated state and parameters directly. For details about how to calculate the square root of the state variance matrix, please refer to Refs[21,22].

### 1.4 Designing the position controller

The position controller of the quadrotor UAV is shown in the dashed box in Fig. 2, which includes 3 independent PD control algorithms.

$$\ddot{x}_r = K_p^x(x_r - x) + K_d^x(\dot{x}_r - \dot{x}) \tag{12}$$

$$\ddot{y}_r = K_p^y(y_r - y) + K_d^y(\dot{y}_r - \dot{y}) \tag{13}$$

$$\ddot{z}_r = K_p^z(z_r - z) + K_d^z(\dot{z}_r - \dot{z}) \tag{14}$$

where $x_r$, $y_r$, and $z_r$ are the referred positions for tracking control. $K_p^x$, $K_d^x$, $K_p^y$, $K_d^y$, $K_p^z$, $K_d^z$ are controller parameters. If the formula 8, 10, and 12 in Eq. (6) are substituted with Eqs(12), (13) and (14) respectively, the first component $U_1$ can be directly obtained, i. e., height controller, as follows:.

$$U_1 = m\sqrt{\ddot{x}_r^2 + \ddot{y}_r^2 + (g - \ddot{z}_r^2)} \tag{15}$$

In addition, according to Eq. (6), it has:

$$\ddot{x}_r = -\frac{U_1}{m}(\sin\phi_r\sin\psi + \cos\phi_r\sin\theta_r\cos\psi) \tag{16}$$

$$\ddot{y}_r = \frac{U_1}{m}(\sin\phi_r\cos\psi - \cos\phi_r\sin\theta_r\sin\psi) \tag{17}$$

The closed solutions[1] of the Euler angles $\phi_r$ and $\theta_r$, as shown in Eq. (18) and Eq. (19), are obtained when Eq. (16) and Eq. (17) are substituted by Eq. (12) and Eq. (13), respectively. In plant application, it is necessary to impose some saturation restrictions on these 2 angles for the arcsine function solution[5].

$$\theta_r = -\arcsin\left(\frac{m}{U_1}(\ddot{x}_r\sin\psi - \ddot{y}_r\cos\psi)\right) \tag{18}$$

$$\theta_r = -\arcsin\left(\frac{m(\ddot{x}_r\cos\psi + \ddot{y}_r\sin\psi)}{U_1\cos\phi_r}\right) \tag{19}$$

### 1.5 Designing the attitude controller

In this paper, the inverse dynamic control method is adopted to design the controller for the attitude subsystem. Now formula 2, 4 and 6 in Eq. (6) are selected and are rewrited in Eq. (20) as the attitude dynamics which will be mainly discussed in the following.

$$\begin{cases} \ddot{\phi} = \dfrac{I_y - I_z}{I_x}\dot{\theta}\dot{\psi} + \dfrac{L}{I_x}U_2 \\ \ddot{\theta} = \dfrac{I_z - I_x}{I_y}\dot{\psi}\dot{\phi} + \dfrac{L}{I_y}U_3 \\ \ddot{\psi} = \dfrac{I_x - I_y}{I_z}\dot{\phi}\dot{\theta} + \dfrac{1}{I_z}U_4 \end{cases} \tag{20}$$

Next, the feedback linearization is used to construct the inverse dynamic controller. First, defining $q = [\phi, \theta, \psi]^{\mathrm{T}}$ for system Eq. (20), controller $u$ is designed as follows:

$$u = M(q)V + h(q, \dot{q}) \tag{21}$$

where $V$ is the virtual input:

$$u = \begin{bmatrix} U_2 \\ U_3 \\ U_4 \end{bmatrix}, \ M(q) = \frac{1}{L}\begin{bmatrix} I_x & 0 & 0 \\ 0 & I_y & 0 \\ 0 & 0 & LI_z \end{bmatrix},$$

$$h(q, \dot{q}) = -\frac{1}{L}\begin{bmatrix} (I_y - I_z)\dot{\theta}\dot{\psi} \\ (I_z - I_x)\dot{\psi}\dot{\phi} \\ L(I_x - I_y)\dot{\phi}\dot{\theta} \end{bmatrix}$$

Through the feedback linearization, Eq. (20) is transformed into a decoupled dual integral linear system. Finally, virtual input $V$ is determined in Eq. (22).

$$V = \ddot{q}_r - K_p(q - q_r) - K_d(\dot{q} - \dot{q}_r) \tag{22}$$

where $K_p$ and $K_d$ are the positive parameters to be tuned. $q_r$ and $\ddot{q}_r$ are the references for the attitude, given by the position subsystem.

## 2 Simulation and comparison

In this section, the flight situation of UAV experiencing the gust is simulated and discussed. By using Matlab, the proposed algorithms are simulated and compared with those without estimation on aerodynamic parameters. The UAV model parameters, as well as controller parameters, used in the simulations, are all referred to the real physical quadrotor system. Table 2 lists all these parameters. Some parameters of UKF algorithm are shown in Table 3.

In the simulation, it is assumed that the quadrotor UAV moves from the starting point $[0 \ \ 0 \ \ 0]^{\mathrm{T}}$ to the endpoint $[10 \ \ 10 \ \ -10]^{\mathrm{T}}$. Assuming that the full states of the UAV except the aerodynamic parameters can be measured with various sensors, such as global position system (GPS) and inertial navigation system (INS). Using the method proposed in this work, the UAV state is augmented by the catenation of the aerodynamic parameters and then jointly estimated by UKF

Table 2 Quadrotor UAV model parameters and controller parameters

| Model parameters | | Controller parameters | |
|---|---|---|---|
| Variables | Value | Variables | Value |
| $m$ | 2.467 kg | $K_p^x$ | 0.15 |
| $g$ | 9.81 N/kg | $K_d^x$ | 0.7 |
| $b_0$ | $2.2893 \times 10^{-5}$ N · s$^2$ | $K_p^y$ | 0.15 |
| $d_0$ | $1.1897 \times 10^{-6}$ Nm · s$^2$ | $K_d^y$ | 0.7 |
| $I_x$ | $5.887 \times 10^{-2}$ kg · m$^2$ | $K_p^z$ | 0.3 |
| $I_y$ | $5.887 \times 10^{-2}$ kg · m$^2$ | $K_d^z$ | 1 |
| $I_z$ | $1.3151 \times 10^{-1}$ kg · m$^2$ | $K_p$ | $[40, 40, 40]^T$ |
| $L$ | 0.3875 m | $K_d$ | $[10, 10, 10]^T$ |

Table 3 Parameters used in the UKF algorithm

| Parameters meaning | Parameters | Value |
|---|---|---|
| Initial variance of the state | $P_0$ | $\begin{bmatrix} 2.5 \times 10^{-6}\boldsymbol{I}_{12} & 0 \\ 0 & 2.5 \times 10^{-12}\boldsymbol{I}_2 \end{bmatrix}$ |
| The variance of the process noise | $Q_w$ | $\begin{bmatrix} 6.25 \times 10^{-8}\boldsymbol{I}_{12} & 0 & 0 \\ 0 & 2.25 \times 10^{-14} & 0 \\ 0 & 0 & 6.25 \times 10^{-16} \end{bmatrix}$ |
| The variance of the measured noise | $Q_v$ | $6.25 \times 10^{-8}\boldsymbol{I}_{12}$ |

**Note**: In Table 3, $\boldsymbol{I}_{12}$ and $\boldsymbol{I}_2$ are unit matrices that have the dimensions of 12 and 2, respectively.

in each interval. The final trajectory is shown in Fig. 3. On the contrary, if only the state of UAV is estimated without time-varying aerodynamic parameters, trajectories are drawn in Fig. 4. During 5 s to 25 s, the UAV goes through gust which causes sudden changes in aerodynamic parameters ($b = 10b_0$ and $d = 10d_0$) as shown in Fig. 5. Using the control method proposed in this work, the UAV attitude during the flight process has a slight fluctuation as shown in Fig. 6. If the aerodynamic

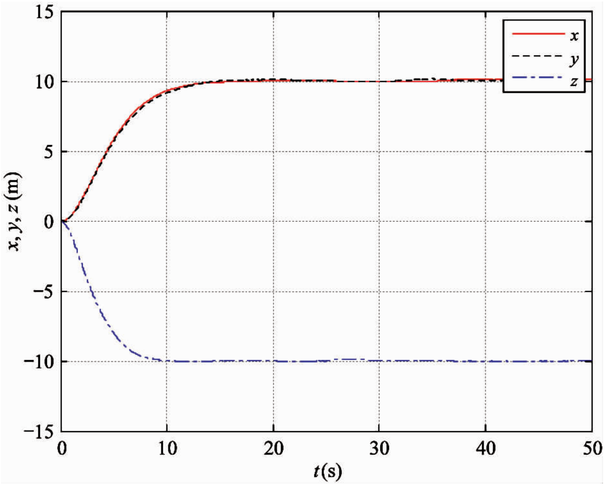


**Fig. 3** The UAV trajectory using the joint estimation on the aerodynamic parameters ($b$, $d$) and the state

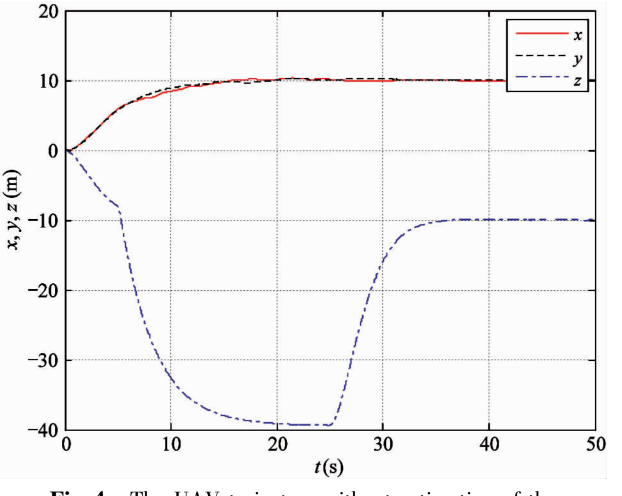


**Fig. 4** The UAV trajectory without estimation of the aerodynamic parameters

parameters are not estimated with the traditional method, the Euler angle experiences a jitter stage as shown in Fig. 7.

Fig. 3 shows that when the aerodynamic parameters are estimated in real time, UAV can reach the target position quickly and steadily and will reach the target point for about 15 s, after which UAV keeps a stable hovering status. Fig. 4 indicates that the control effect of UAV is poor when there is no real-time estimation of the aerodynamic parameters. Specifically, UAV shows a strong divergence trend in the height control on the wind disturbance emergence from time $t = 5$ s. This trend continues till the disturbance cancellation ($t = 20$ s) at which the height deviation is intolerable for any practical application.

Fig. 5 is the aerodynamic parameters curve. It can be seen from the figure that the estimated value is very close to the actual value. This indicates that the UKF algorithm has a good estimation accuracy. Comparing Fig. 6 and Fig. 7, UAV shows good stability in the attitude when there exists parameter online estimation, and there is violent fluctuation when without parameter estimation. When there is a real-time estimation of the aerodynamic parameters, the UAV will fluctuate with attitude slightly (about 1 °) only when the uncertainty suddenly occurs ($t = 5$ s), and the attitude angle will continue to converge to the steady state quickly. In contrast, when the aerodynamic parameters estimation is not considered, even if the wind disturbance disappears, the UAV will still fluctuate violently. The max fluctuation will be greater than 6 °.

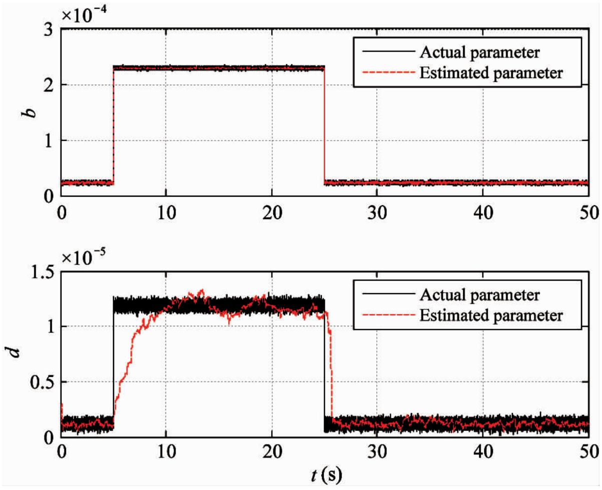


**Fig. 5** The actual aerodynamic parameters and their estimation

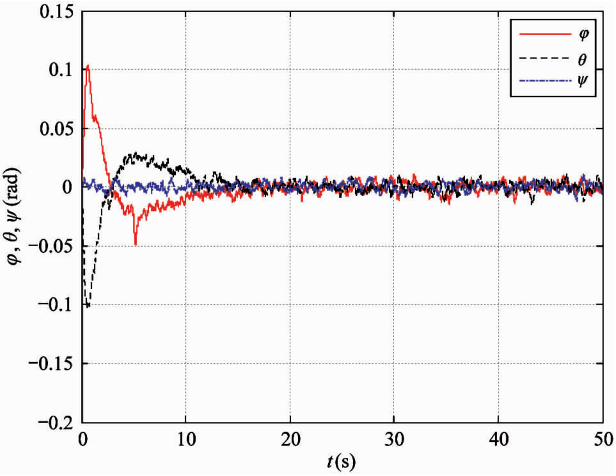


**Fig. 6** Euler during UAV flight with the proposed method

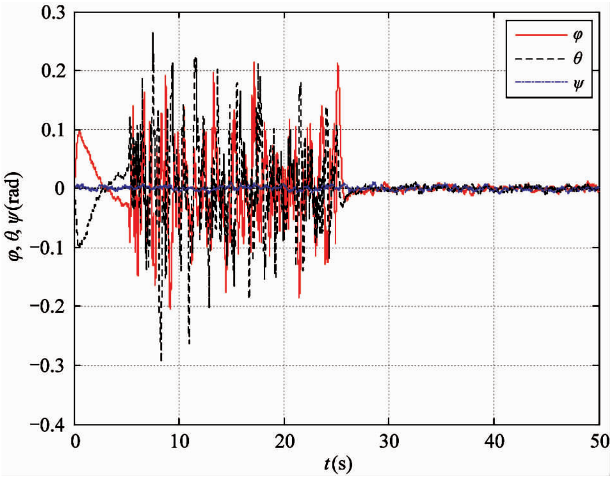


**Fig. 7** The Euler of the UAV in the flight process without parameter estimation

## 3 Conclusions

The uncertainty of wind disturbance causes great difficulties for the control precision of the quadrotor UAV. In fact, the thrust coefficient and the reaction torque coefficient of the rotors act as a link between the vehicle and external environment. In order to consider the time-varying effects, this paper proposes an online joint estimation of the aerodynamic parameters of the rotors. Based on a control structure with 2 embedded loops, the UAV position controller and the attitude controller are designed separately. Various simulations indicate that the proposed control scheme is feasible and can effectively overcome the influence of the time-varying disturbance. Compared with the method without aerodynamic parameters estimation, the proposed method has better reliability and control precision.

**References**

[1] Wang H, Ye X, Tian Y, et al. Model-free-based terminal SMC of quadrotor attitude and position [J]. *IEEE Transactions on Aerospace and Electronic Systems*, 2016, 52(5):2519-2528

[2] Mellinger D, Shomin M, Michael N, et al. Cooperative Grasping and Transport Using Multiple Quadrotors [M]. Berlin-Heidelberg: Springer, 2013: 545-558

[3] Antonelli G, Cataldi E, Arrichiello F, et al. Adaptive trajectory tracking for quadrotor MAVs in presence of parameter uncertainties and external disturbances [J]. *IEEE Transactions on Control Systems Technology*, 2018, 26(1): 248-254

[4] Hancer C, Oner K T, Sirimoglu E, et al. Robust position control of a tilt-wing quadrotor [C]//Proceedings of the 49th IEEE Conference on Decision and Control, Atlanta, USA, 2010: 4908-4913

[5] Sydney N, Smyth B, Paley D A. Dynamic control of autonomous quadrotor flight in an estimated wind field [C]//Proceedings of the 52nd IEEE Conference on Decision and Control, Florence, Italy, 2013: 3609-3616
[6] Waslander S L, Wang C. Wind disturbance estimation and rejection for quadrotor position control [C]//AIAA Infotech@ Aerospace Conference and AIAA Unmanned Unlimited Conference, Seattle, USA, 2009: 1-14
[7] Escareño J, Salazar S, Romero H, et al. Trajectory control of a quadrotor subject to 2D wind disturbances [J]. *Journal of Intelligent & Robotic Systems*, 2013, 70(1-4): 51-63
[8] Wang C, Song B, Huang P, et al. Trajectory tracking control for quadrotor robot subject to payload variation and wind gust disturbance [J]. *Journal of Intelligent & Robotic Systems*, 2016, 83(2): 315-333
[9] Abeywardena D, Wang Z, Dissanayake G, et al. Model-aided state estimation for quadrotor micro air vehicles amidst wind disturbances [C]//Proceedings of the IEEE/RSJ International Conference on Intelligent Robots and Systems, Chicago, USA, 2014: 4813-4818
[10] Rigatos G, Siano P. Control of quadrotors with the use of the derivative-free nonlinear Kalman Filter [J]. *Intelligent Industrial Systems*, 2015, 1(4): 275-287
[11] Nobahari H, Sharifi A R. Continuous ant colony filter applied to online estimation and compensation of ground effect in automatic landing of quadrotor [J]. *Engineering Applications of Artificial Intelligence*, 2014, 32: 100-111
[12] Mercado D, Castillo P, Castro R, et al. 2-sliding mode trajectory tracking control and EKF estimation for quadrotors [J]. *IFAC Proceedings Volumes*, 2014, 47(3): 8849-8854
[13] Lei W, Li C. On-line aerodynamic identification of quadrotor and its application to tracking control [J]. *IET Control Theory & Applications*, 2017, 11(17): 3097-3106
[14] Ma D, Xia Y, Li T, et al. Active disturbance rejection and predictive control strategy for a quadrotor helicopter [J]. *IET Control Theory & Applications*, 2016, 10(17): 2213-2222
[15] Izadi H A, Zhang Y, Gordon B W. Fault tolerant model predictive control of quad-rotor helicopters with actuator fault estimation [J]. *IFAC Proceedings Volumes*, 2011, 44(1): 6343-6348
[16] Sakamaki J Y, Beard R W, Rice M D. Cooperative estimation for a vision-based target tracking system [C]//Proceedings of the International Conference on Unmanned Aircraft Systems (ICUAS), Arlington, USA, 2016: 878-885
[17] McKinnon C D, Schoellig A P. Unscented external force and torque estimation for quadrotors [C]//Proceedings of the IEEE/RSJ International Conference on Intelligent Robots and Systems (IROS), Daejeon, Korea, 2016: 5651-5657
[18] Ireland M, Vargas A, Anderson D. A comparison of closed-loop performance of multirotor configurations using non-linear dynamic inversion control [J]. *Aerospace*, 2015, 2(2): 325-352
[19] Nagaty A, Saeedi S, Thibault C, et al. Control and navigation framework for quadrotor helicopters [J]. *Journal of intelligent & robotic systems*, 2013, 70(1-4): 1-12
[20] Bouabdallah S. Design and Control of Quadrotors with Application to Autonomous Flying [D]. Tlemcen: Ecole Polytechnique Federale de Lausanne, 2007
[21] Wan E A, Merwe R V D. The unscented Kalman filter for nonlinear estimation [C]//Proceedings of the IEEE 2000 Adaptive Systems for Signal Processing, Communications, and Control Symposium, Lake Louise, Canada, 2000: 153-158
[22] Merwe R V D, Wan E A. The square-root unscented Kalman filter for state and parameter-estimation [C]//Proceedings of the IEEE International Conference on Acoustics, Speech, and Signal Processing, Salt Lake City, USA, 2001, 6: 3461-3464

**Yang Yanhua**, born in 1983. She received her Ph. D degree at State Key Laboratory of Robotics, Shenyang Institute of Automation, Chinese Academy of Sciences in 2014. She also received her B. S. and M. S. degrees from Fuzhou University in 2004 and 2007, respectively. She has worked in Wuhan University of Science and Technology. Her research interests include mobile robot control, teleoperation, and robust control.